Geological Quarterly, 2021, 65: 24
DOI: http://dx.doi.org/10.7306/gq.1592

Soil development in a coal-burning environment: the Upper Silesian waste heaps of Poland

Łukasz KRUSZEWSKI[1, *], Monika KISIEL[2] and Małgorzata CEGIEŁKA[1]

[1] Polish Academy of Sciences, Institute of Geological Sciences, Twarda 51/55, 00-818 Warszawa, Poland

[2] Cardinal Stefan Wyszyński University, Institute of Biological Sciences, Wóycickiego 1/3, 01-938 Warszawa, Poland

Kruszewski, Ł., Kisiel, M., Cegiełka, M., 2021. Soil development in a coal-burning environment: the Upper Silesian waste heaps of Poland. Geological Quarterly, 65: 24, doi: 10.7306/gq.1592

Soil development in burning coal-mining waste heaps is a rarely addressed phenomenon, especially in Poland and in relation to pyrometamorphic substrates. Eight samples were collected from 5 heaps, four of them obtained from Europe's highest "Szarlota" heap located in Rydułtowy. Traces of pedogenesis were observed in both thermally changed (pyrometamorphic) and megascopically unchanged substrates. Grain size distribution is variable, with the finest silt being most clearly associated with distinct, though modest, trace element (TE) enrichment, primarily of Sb, As and Pb, and Ba and Cu. Slight variations in soil mineralogy occur even in samples derived from various parts of the "Szarlota" heap. Goethite, however, is a frequent component in most samples studied; it is an important pedogenesis factor in the soils studied and seems to be correlated with salinity. To some extent, it also influences TE composition. Relatively invariable pH, moderate TE and nutrient contents, and a lack of Al_w allows vegetation growth at most of the locations studied.

Key words: coal mining waste, soil geochemistry, burning heaps, weathering, pyrometamorphic materials.

INTRODUCTION

Coal mining produces large volumes of waste, deposited mainly in burning coal-mining waste repositories (BCWRs, also known as heaps, dumps, piles, gobs, and bingsteads) which are found throughout the world, (e.g., Srebrodolskiy, 1989; Žáček et al., 1995; Witzke, 1996; Sokol et al., 2005; Szabó et al., 2015). They contain coal remnants, barren shales and sandstones, carbonate concretions; and other rock types.

Both the coal-containing waste materials located within the post-mining heaps and the coal deposits themselves (e.g., Kim, 2007) can be subject to coal fires, a worldwide phenomenon associated with coal self-heating, self-ignition and combustion. Coal organic matter oxidation, the formation of oxocarbons, coal petrology, the physico-chemistry of coal macerals, and the catalytic role of iron sulphides are fundamental factors of the coal combustion process (e.g., Wagner, 1980). Spontaneous coal combustion is considered to be a primary cause of coal fires in BCWRs (e.g., Nelson and Chen, 2007). Initiation of these fires is influenced by air access, waste material compaction, and dump shape.

BCWRs are objects where intense mineralization occurs due to transformations of the coal itself, and of the waste rocks and associated barren rocks (e.g., Srebrodolskiy, 1989).Three types of mineralization are known, produced by three distinct fire-induced processes: (1) high-temperature pyrometamorphism, occurring at the burnout stage, leading to formation of clinkers, buchites, parabasalts, and slags; (2) medium-temperature exhalative processes within the surface and subsurface zones of fumaroles (or pseudofumaroles), including gas condensation and gas-waste interaction similar to pneumatolysis; and (3) low-temperature supergene alteration (weathering) of waste material (Srebrodolskiy, 1989; Nasdala and Pekov, 1993; Stracher, 2007; Kruszewski, 2013a). Although BCWRs are of anthropogenic origin, the mineral-forming processes occurring within them are usually natural. Although >200 CWR located in the Upper Silesian Coal Basin (USCB) alone (Ł. Gawor, 2017 pers. comm.) are currently not burning, self-heating processes may still be taking place.

Coking and pyrolysis lead to formation of a number of gaseous species that constitute the BCWR gaseous transfer medium. Coal-fire gas composition was studied in detail by Kruszewski et al. (2018, 2019) based on numerous USCB BCWR vents. The main components are variably enriched in CO_2 and H_2O, followed by usually minor CH_4. The N-rich gases are represented predominantly by NO_2 and NH_3, with an important addition of HCN and isocyanic acid and less frequent NO, acrylonitrile, pyridine, and N_2O. The essential S-bearing gases are thiophene (C_4H_4S) and dimethyl sulphide, with some H_2S, dimethyl disulphide, SO_2, and traces of SF_6. The primary Cl-rich gases are haloalkanes (mainly 1,1-dichloroethane and dichloromethane) followed by haloalkenes, other halocarbons, HCl, and CCl_4 (and possible $GeCl_4$). AsH_3, SiF_4, phenol, *o*-cresol, oxy-organics (furan, tetrahydrofuran), acetic and formic acids, alcohols, aldehydes, ketones, esters, and amines

* Corresponding author, e-mail: lkruszewski@twarda.pan.pl

Received: December 15, 2020; accepted: March 29, 2021; first published online: June 9, 2021

were also detected. Another product of coal decomposition, thermally altered organic matter, comprises Polycyclic Aromatic Hydrocarbons (PAHs), various nitro-organics, thiophene and other S compounds, phenols, and other compounds.

BCWRs IN POLAND – THE STATE OF THE ART

There are numerous papers concerning BCWRs in Poland which examine different aspects of them:. pyrometamorphic processes and related minerals (e.g., Kruszewski, 2008, 2013a); mineralogy and gas geochemistry related to exhalative processes (e.g., Kruszewski et al., 2018, 2019); the distribution and composition of coal-derived materials in the local environment (Nowak, 2011; Nádudvari et al. 2018); thermal transformation of coal organic matter in local BCWRs (Misz-Kennan and Fabiańska, 2010); PAH assemblages (e.g., Kuna-Gwoździewicz, 2013); supergene mineralization (Kruszewski, 2013a); and fire hazards in BCWRs (e.g., Drenda et al., 2007; Różański, 2018). In addition, several papers note a large range of physico-chemical conditions in BCWRs making them attractive models for various terrestrial and extraterrestrial environments (e.g., Kruszewski et al., 2017).

Element availability in soils is governed mainly by the soil pH, especially as regards microelements. The most important elemental forms in soils are Ca^{2+}, Mg^{2+}, K^{+}, Na^{+}, NH_4^{+}, and NO_3 (Norton and Ouyang, 2019). Water-insoluble compounds of the main elements form a nutrient reserve, gradually released during weathering. Organic N (from humus and plant remains) may represent as much as 99% of the total N. Plants uptake N as either NO_3 or NH_4 . At C/N ratio above 33:1, the amount of plant-available N is lowered. At C/N <17:1, N is readily mineralized and thus more available. Typical C:N values in soil humic horizons are ~10:1. The next important macroelement is P, which governs plant flourishing, seed formation, ripening, and disease resistance. The plant-available form corresponds to up to 80 ppm of total P content (Zawadzki, 1999; Mocek, 2015). Many of the plant physiological functions are potassium-dependent. The plant-available form of K usually represents up to 2% of its total content and is equal to K^{+} ions sorbed by soil, and soil solutions (Raghad et al., 2016). The latter two sinks are also important for Ca, Mg, and Na availability. Calcium both influences plant physiology and works against soil acidification. Magnesium is an essential enzymatic activator and photosynthesis factor in plants. Iron influences plant physiology (Hänsch and Mendel, 2009). Iron oxyhydroxides participate in the formation of exchangeable sorption capacity and soil structure. Sulphur has a structural role in proteins, photosynthesis and oxidative-reductive tissue processes. The sulphate form is available for plants and represents up to a few % (up to 50 ppm) of the total S. Normal plant growth is also dependent on Cu, Zn and Mn contents. Molybdenum is used by plants in nitrate-to-ammonia reduction, atmospheric N_2 fixation (along with Co) and soil P transformations. Other trace elements (TEs) are not essential to plants but may be toxic. This is true of the major element Al (Bhatla and Lal, 2009; Mocek, 2015).

Although little is known regarding soil formation in BCWRs, a number of studies either of the influence of coal mining on soils or soil remediation in such mining areas have been made. The studies carried out on plant-remediated CWRs suggest that they can be a sink for CO_2 emissions (Tripathi et al., 2014), although this does not seem to be true for the CWRs affected by fires (e.g., Kruszewski et al., 2018).

Acidic soils, as observed in an Indian CWR by Upadhyay et al. (2016), owe their acidity to coal waste decomposition. According to Meuser (2013) this also has to do with the scarcity of texture-forming large particles, and lack or scarcity of clay and humic fractions, as well as high infiltration rates and hydraulic conduction. The soils of German CWRs are known to be dry, thus limiting root development. Slope characteristics of a CWR are variable, but both outer and inner escarpments are very steep (sometimes vertical in the case of the inner escarpments). This makes CWR soils susceptible to erosion, which leads to less well developed soil structure. Black soils undergo intense heating in summer, with ground temperatures locally reaching 70°C, and such overheating is greatly exacerbated by internal and ground fires. A frequently addressed issue related to CWR soils is their hydrophobicity Meuser (2013). Technosols with such characteristics were studied, e.g., by Atanassova et al. (2018) in a dump related to the Marit-Iztok mine, SE Europe. The general soil characteristics in this case include elevated bioavailability of metals, low moisture, water repellence, and a higher sand content than in the case of a pine-vegetated soil example. The authors suggested a common source of soil hydrophobicity and soluble/exchangeable forms of Co, Cu, Fe, Mn, Ni, Pb, and Zn. The metals listed – except for Pb – are positively correlated with sand fraction content. The soil organic matter that includes elevated levels of PAHs is more chemically inert than its counterparts from wettable hydrophilic soils.

Some German CWR soils are reported to show nutrient deficiency, with low P (e.g., mean 200 ppm), low C (organic matter content), and low N. The amount of K^{+} and Mg^{2+} is, though, reported to be sufficient at 70 and 60 ppm, respectively (Meuser, 2013). The occurrence of pyrite and chalcopyrite in the waste leads to oxidative formation of SO_4^{2} and Fe, and also to a drop in pH to values of 1.8–2.5. The related acid mine drainage (AMD) in the coal area of Tula, Russia leads to heavy metal release and slight soil enrichment in Cu, Co, Ni, Pb, and Zn (Meuser, 2013). According to this author, higher levels of metals in hard-coal heaps are normally not detected, and the contents of Cu, Pb, Ni, and Zn in the Ruhr case are as follows: <50 ppm, <30 ppm, <80 ppm, and <70 ppm.

Jiang et al. (2014) has indicated cadmium (max. 0.18 ppm content) as the highest-risk element contained in a coal-gangue dump in Jilin, China. Querol et al. (2011) studied a BCWR in the Datong area in China. They reported quartz, feldspars, kaolinite, hematite, illite, calcite, amphiboles, and occasionally also cordierite, goethite, and augite in condensate-hosting soils. The compositions of the coal studied (pH 6.1), shale (pH 6.7) and clinker (pH 6.3 and 6.4) leachates, respectively, are [in ppm]: <3, 33, <3 Al; 396, 8, 92 and 7400 Ca; <1, 1.5, and <1 Fe; <3, 100, 65 and 109 K; 106, 2, 6 and 78 Mg; 26, 51, 28 and 107 Na; <5 P; 9, 105, 24 and 43 Si; 1, 4, NH_4 ; 1072, 133, 252 and 16600 SO_4^{2} ; 66, 78, 60 and 74 Cl^{-}. Not only the waste deposition, but also the coal-mining in general, affects soils. Arefieva et al. (2019) studied the influence of mine waters on mine area soils in the Partizansk area, Russia. The soils studied showed pH variations of 5.8–8.5. Highly disturbed soils are shown to represent an environment of fluctuating pH, texture, salinity, sodicity, and soil stability. Changing pH is troublesome due to B, Cd, Cu, Mo, Se and Zn availability. Low pH favors leaching of B, Ca, K and N. A rise in salinity is, in turn, a factor lowering water availability (Iverson and Wali, 1992).

Awoyemi and Dzantor (2017) pointed to coal fly ash (CFA) as an important source of heavy elements in soils located in coal-mining areas. Their study showed increase in As (from 0.20 to 7.7 ppm), and minor rises in Cu, Zn, Cr, and Cd in soil experimentally contaminated with CFA. CFA emissions are also observed in the USCB BCWR fumaroles, but our initial data does not show marked elemental enrichment apart from Hg. Coal itself is also a well-known sink of TEs. Typical mean concentrations in USCB coals are [ppm]: 5.1 As, 0.68 Cd, 77

Pb, 1.0 Sb, 111 Zn (Smoliński et al., 2014); 50 As (Juda-Rezler and Kowalczyk, 2013); 1.1 Cd, 45 Co, 42 Ni, 42 Pb, 62 Zn (Parzentny and Lewińska-Preis, 2006). Our unpublished data shows mean Hg concentrations in USCB shales being as much as 17 ppm – a high value. Mercury soil flux derived from coal fires in the strongly burning Wuda coalfield, China, was assessed by Li et al. (2018). The concentrations noted above, however, pale in comparison to the extreme concentrations seen in some coals elsewhere, like those of Ge in the Spetsugli ("Special Coals") and those of Sb in the Vanchinsk deposits in Russia. There are many other examples of such kind (Seredin and Finkelman, 2008).

Fires influence soil properties. The study of de Rouw (1994) conducted on Ivory Coast's poor soils shows that fire induces organic matter mineralization and acidity drop due to ash formation. Fires also diminish toxic Al activity in the soil and raise nutrient availability. Nitrogen and oxygen are prone to be lost in the course of fires by volatilization. Soil heating also largely increases the solubility of N-organics (Knicker, 2007). Martinez and Ressler (2001) studied soils in the famous Centralia ghost town where local temperatures were measured to be as high as 119°C. They indicate fumarole-derived NH_3 and possibly other gases as the source of NO_3 and of other soil nutrients such as PO_4^3 .

To our best knowledge, the only two papers investigating soils on Polish BCWRs are those of Zając and Zarzycki (2013) and Abramowicz et al. (2021). Those authors, however, focus more on plant development than on soil properties. Another study in the USCB concerns anthropogenically-altered surface soil layers adjacent to the Niwka-Modrzejów mine in Sosnowiec (Cabala et al., 2006). Klatka et al. (2019) studied soils in a post-mining area adjacent to the "Ruch-Borynia" mine in the Jastrzębie area of the USCB.

The current study is a pilot one. Its main goal is to report soil development and soil geochemical characteristics in zones dominated by pyrometamorphic (PM) rock units with clinkers being the main metamorphic rocks. These zones may compromise as much as 50% of the total BCWR volume. Numerous non-anthropogenic, coal-fire-related PM sites are known worldwide (Sokol and Volkova, 2007). However, the soil development in such geochemically and mineralogically aberrant zones is not well understood. Novikova et al. (2015) reported loamy soils covering large pyrometamorphic bodies in the Kuznets Coal Basin. An example profile of a younger such body has an upper, ~20 cm thick soil covering subaerial loam. Both these layers cover an undisturbed clinker zone, ~2.5 m thick, partially covered by red weathered rock (~1.2 m thick). The latter is also locally overlain by ~1.3 m thick layer of redeposited rocks. The pyrometamorphic rocks overlie "modern soil and sward" and are usually only weakly altered. Unfortunately, no other soil properties were discussed by these authors.

STUDY SITES

Soil samples were collected in 5 BCWRs of the USCB. The location of the basin in Poland and of the objects studied is shown in Figure 1. The collection sites, including plant coverage data, are detailed in Table 1. Most of the samples were taken from surface of local pyrometamorphic bodies that are both mineralogically and geochemically specific to the coal-burning environment. Four of the objects probed were closely studied by one of us (Ł.K.).They include "Szarlota" heap in Rydułtowy, the highest in Europe, the nearby "Wrzosy" heap in Pszów and the "Marcel" mine heap in Radlin. These three heaps are located within the Rybnik Coal Region and all are currently thermally highly active.

The "Szarlota" heap was probed in 4 places to show potential soil variability within virtually identical pyrometamorphic bodies, samples RDT1g, RDT2g, and RDT3g being taken from apical parts. The RDT1 site bears some dry perennials though minor young birches and a single, tiny pine were observed nearby. Here, clearly weathered clinker forms a cover (<5 cm thick) directly on the pyrometamorphic rocks. Adult birches are the only plants macroscopically observed at the RDT2 site. This site's soil, macroscopically different from that found at the former site, was taken from in between the complex rhizosphere of a single tree. The RDT3 site is on the eastern foothill of the high conical pile; only a few *Verbascum* grow there. Neither typical soil cover nor weathering were observed at that point. Sample RDT4g was collected from the nearby upper part of a slope composed of the same pyrometamorphic material (pile), the bottom of which was probed at the RDT1 point. It is located immediately above an active fumarolic system, where the mineral and organic pyrolysate geochemistry was studied by Kruszewski et al. (2018). A local crack with visible pyrometamorphic materials seems to be surrounded by a very thin (<5 cm), dark humus layer, covered by mosses. In Pszów, the soil sample was collected at the foot of the heap, on its eastern side, and its geological profile resembles that of the RDT4 site, although with partially weathered black shales evident. Dry perennials, similar to those at the RDT1 site, grow here. The RD1 site most closely resembles RDT2 in both geology and botany, although without clear traces of weathering or pedogenesis. The RSH1 site, located at the foothill of the currently thermally inactive "Halemba" mine heap in Ruda Śląska, is also geologically similar to the RDT2 (and RD1) sites. However, trees and other plants grow here in both the ground and on separate blocks of pyrometamorphic breccia lying on the ground. The RSH1 sample was collected from such a block, from between roots of a birch and other broadleaf trees (e.g., *Populus*), the roots being surrounded by mosses. The ZBB1 soil sample comes from an organic-pyrolysate-rich fire zone of the "Ruda" heap in Zabrze (Biskupice district). The zone geochemically differs from all the remaining samples as it represents the only niche at an active organic fumarole. The fumarole organic deposits (thermally altered organic matter) include visible sulphur crystals. No pyrometamorphic rocks are present here. Salammoniac (NH_4Cl) crystals are also seen in places, being leached out during rain.

The thickness of soil cover at many sample spots does not exceed 10 cm. No evident allogenic soils were observed at collection spots RDT1, RDT2, RDT3, RD1 and RSH1. Thin humic levels at PS1 and RDT4 also seem to be of authigenic origin. The only site where some allogenic material could possibly have been deposited is that of ZBB1. However, its barren geochemical character, as shown below, seems to contradict this possibility.

RESEARCH METHODS

MINERALOGICAL PHASE ANALYSIS

Powder X-Ray diffraction (PXRD) was used to determine the mineralogical composition of the exhalative mineral mixtures, in qualitative and quantitative phase analysis. Samples were crushed and ground in an agate mortar. The PXRD analyzes were conducted using a Bruker axs *D8 ADVANCE* diffractometer at the Clay Minerals Laboratory, Institute of Geo-

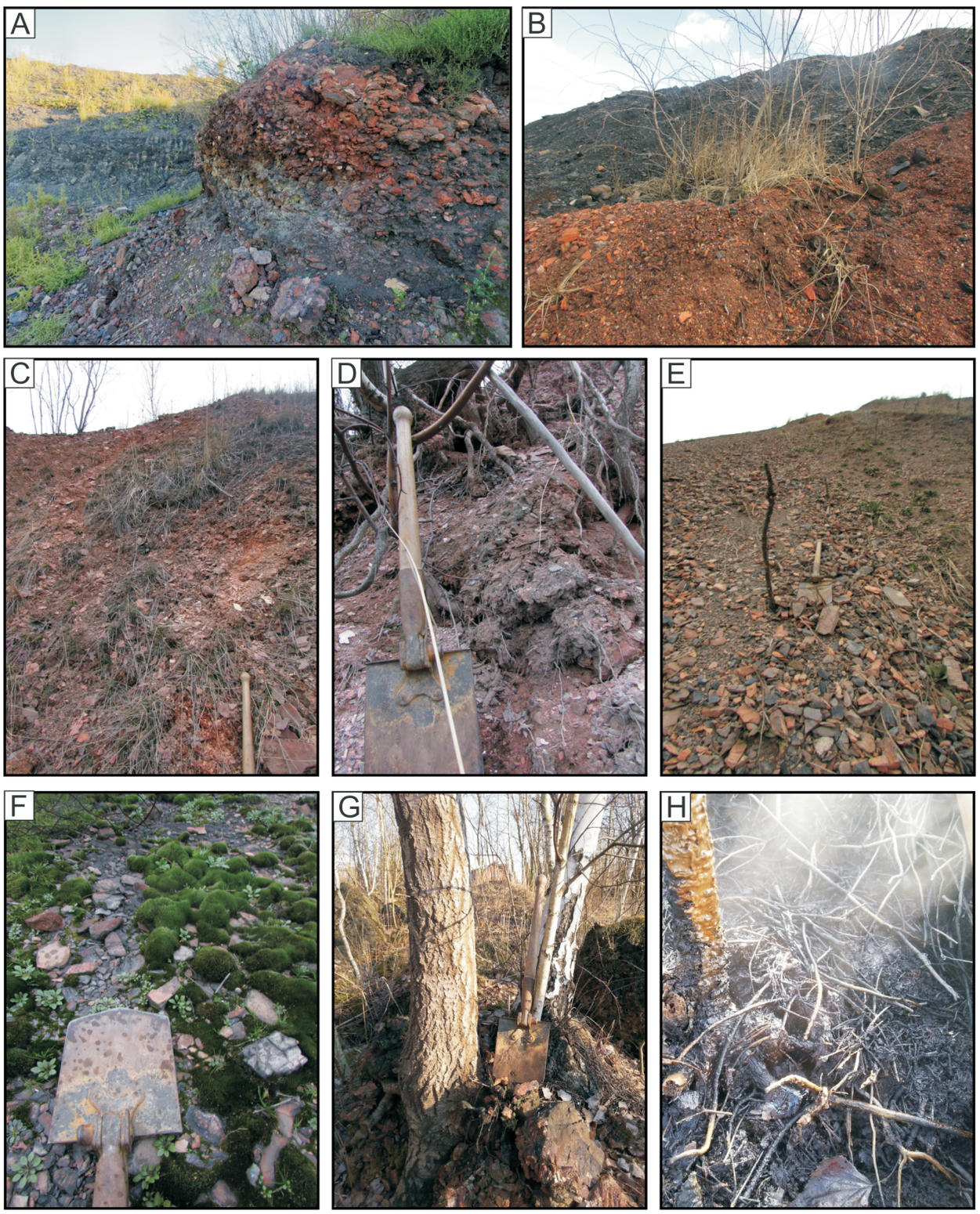

Fig. 1. View of soil sampling points

A – Wrzosy heap, Pszów; **B** – heap of the Marcel coal mine, Radlin; **C**–**F** – Szarlota heap in Rydułtowy, sites 1, 2, 3 and 4, respectively; **G** – heap of the Halemba coal mine, Ruda Śląska; **H** – Ruda heap in the Biskupice district of Zabrze

Table 1

Location and general geological description of the sampling points

Sample	City	Heap name	Heap size [ha]	Latitude	Longitude	Geology	Plant coverage
PSg1	Pszów	Wrzosy	20.1	50°02'42" N	18°25'22" E	weathered coaly shales on thin PM unit	dry perennials
RD1g	Radlin	unnamed	19.3	50°02'22" N	18°28'39" E	PM unit	dwarf *Betula* L.
RDT1g	Rydułtowy	Szarlota	37.8	50°03'49" N	18°26'27" E	PM unit with weathering cover	dry perennials, dwarf *Betula* L., single dwarf pine
RDT2g	Rydułtowy	Szarlota	37.8	50°03'49" N	18°26'34" E	PM unit; weathering cover; rhizosphere	*Betula* L. (relatively rich coverage)
RDT3g	Rydułtowy	Szarlota	37.8	50°03'43" N	18°26'26" E	PM unit	*Verbascum*
RDT4g	Rydułtowy	Szarlota	37.8	50°03'40" N	18°26'22" E	thin organic cover of a clinker-rich PM unit; a fumarole	mosses; dwarf trees in the vicinity
RSH1g	Ruda Śląska	unnamed	unknown	50°14'38" N	18°51'49" E	old PM unit with clinker and buchite	large trees, locally mosses, *Oenothera biennis*, *Taraxacum officinale*
ZBB1g	Zabrze	Ruda	35	50°02'22" N	18°28'39" E	organic fumarole, bitumen-rich	dead dwarf trees (*Betula* L., pine); *Solanum nigrum*

logical Sciences, Polish Academy of Sciences, Kraków. The apparatus was equipped with a superfast LPSD VÅNTEC-1 detector and used non-monochromatized, k -filtered CoK radiation. The following parameters describe the analysis conditions: Bragg-Brentano geometry, 3-80 2 range, 0.02 2 step, 1s/step counting time, no monochromatization. TOPAS (v. 3.0) with Rietveld method (Rietveld, 1967) were used for the qualitative phase analysis. The approach used was tested via attendance in the Reynolds Cup 2018 competition (Ł.K.) and details of it may be found in Kruszewski (2013a).

BULK GEOCHEMISTRY

Bulk geochemistry (main and selected trace elements) of powdered samples was determined using the Inductively Coupled Plasma E Spectroscopy (ICPES) method at ACME Labs (Bureau Veritas), Canada. Due to the content of refractory minerals such as spinel and mullite a multi-acid digestion package was selected. In this package, a 0.25 g sample split is dissolved in a heated mixture of HNO_3, $HClO_4$, and HF, the residue being dissolved in HCl. A CHNS elemental analyzer was used to measure the contents of these four elements. The good quality of the ICPMS and CHNS analyzes is indicated by a very clear linear correlation between the sulphur content measured by ICPMS and CHNS.

PEDOLOGICAL PARAMETERS

The description of the soil profiles was prepared according to the requirements of the Polish Society of Soil Science (Kabała et al., 2019). Soil colour was determined using Munsell Soil Color Charts. Determinations of the basic soil properties were made according to the standards used in soil science (Karczewska and Kabała, 2019): particle-size distribution (PSD) using the Casagrande method with the modification of Prószyński, pH of soil in H_2O and in 1M KCl using the electrometric method, exchangeable acidity (EA) which was extracted with unbuffered 1 M KCl (soil:solution 1:10), and titrated potentiometrically up to pH 7.8. Exchangeable aluminum (Al_{ex}) was measured in the same extract by potentiometrical titration, indirectly, after aluminum precipitation using NaF. Measurements of the exchangeable base cations Ca, Mg, K, Na using ammonium acetate extraction at pH = 7 were conducted using a *Shimazu ICPE-9820* plasma spectrometer.

Carbonate content class was reported based on the intensity of the earth part reaction with 10% HCl. Porewater composition was not analysed but it is expected to be enriched in Cl^- and SO_4^{2-} by analogy with data from Pałys (1966), Pluta et al. (2012), Arefieva et al. (2019) and Querol et al. (2011). Enrichment factors were calculated by dividing the values obtained values by published values, as explained in the Discussion.

DATA TRANSFORMATION

The data was analysed using Pearson correlation within biplots. The data was also log ratio-transformed. The observed correlations for all log ratio-transformed intra-dataset values were tested using the Mann-Whitney nonparametric relevancy test (Lehmann, 1975) with t-Student values derived from tables. The confidence interval = 0.05 was used. Herein we exclusively refer to Pearson correlation factors that have positively passed the above test.

RESULTS

SOILS BULK GEOCHEMISTRY

Results of the bulk soil geochemistry (main and trace elements) analyses, by ICP, are given in Table 2. Results of the bulk soil elemental CHNS analyses are given in Appendix 1*. The results are explained in the Discussion section.

MINERAL COMPOSITION OF THE SOILS

Results of the quantitative phase analyses of the soil samples are given in Table 3. Ba and Mn are treated as trace elements here, because they do not enter most mineral phases as

* Supplementary data associated with this article can be found, in the online version, at doi: 10.7306/gq.1592

Table 2

Results of CHNS bulk elemental analysis (in wt.%) and ratios in the soil samples

Sample	C[1]	H	N[1]	S	C/N	C/H
PS1g	6.62	0.85	0.30	0.25	22	8
RD1g	6.96	0.56	0.15	0.62	46	12
RDT1g	2.58	0.55	0.17	0.26	15	5
RDT2g	5.58	0.91	0.39	0.85	14	6
RDT3g	5.92	0.94	0.20	0.23	29	6
RDT4g	**12.79**[2]	**1.23**	0.37	**1.52**	35	10
RSH1g	**18.81**	1.75	0.63	0.21	30	11
ZBB1g	**14.23**	1.47	1.42	4.40	10	10
Geometric mean	7.78	0.96	0.34	0.57	22	6

[1] typical soil concentration: 0.020.35 (mineral soils), 14% (organic soils), of which 15% stands for NH_4 and/or NO_3 forms (Mocek, 2015); [2] – outstanding values are given in bold

main components (Kruszewski, 2018). Most R_{wp} values are below 10% and all GOF (goodness of fit ^{2}) values are <2 which indicates a good fit quality in general. Clear glass is present in samples RD1g and RSH1g only. For these samples' refinements the GOF values are slightly lower due to a better fit related to glass inclusion in the refinement in the form of a Peaks Phase, i.e., to derive the amorphous phase content. Most samples studied have relatively low quartz content (around 20 wt.%), with the otherwise organic-rich ZBB1g sample being the only one with quartz content >50 wt.%. Illite content is usually in the 30–41 wt.% range (most typically in pyrometamorphic samples). Both illite and kaolinite contents are lower in sample RD1g due to its evident higher level of protolith thermal transformation, as further attested by elevated levels of the typically pyrometamorphic minerals anorthite, mullite, and hematite. All other samples except for ZBB1g show relatively similar kaolinite contents of 11–14 wt.%. The chlorite-group content is also quite consistent in most samples (3–6 wt.%) while being absent from samples RD1g and ZBB1g: in sample RD1g any chlorite was destroyed due to greater thermal transformation while for both samples a Mg-low protolith also explains the chlorite absence. The K feldspars, both orthoclase and microcline, show similar contents in all of the samples studied samples, at 1–4 wt.%, with very slightly elevated content in sample PS1g. The PXRD characteristics of plagioclase among the samples are slightly variable, suggesting the presence of albite in the RDT samples and anorthite in the remaining ones. The Rybnik area samples (RDT, RD, PS) show higher plagioclase abundance. Hematite is present in all samples except for ZBB1g. Indialite – a typical pyrometamorphic mineral – acts as a minor component in samples RD1g and RSH1g. Its low abundance is due to the lack of buchite and parabasalt rocks in the C soil level (indialite is a discriminative component of these two rock types). There are also traces of cristobalite, in sample RSH1g only; a highly elevated mullite content in this sample seems to reflect a more aluminous protolith character. Gypsum is relatively abundant, being confirmed in half of the samples studied; it is common on the surfaces of pyrometamorphic rocks on USCB heaps, as observed *in situ* by Ł.K.

Goethite is present in 5 of 8 samples studied and, besides the clay minerals, is the only weathering species indicating pedogenic processes (e.g., Schwertmann, 1971). Jarosite occurs in sample RDT3g, which has the best-developed rhizosphere. Jarosite accumulations surrounding tree rhizomes were also observed by one of us (Ł.K.) in another heap. Goethite is virtually absent from samples RDT1g, RSH1g, and ZBB1g, although its presence may be misrepresented due to small crystallite size.

PEDOLOGICAL AND RELATED PARAMETERS

The pedological analysis results are shown in Table 4. The pH values as measured in H_2O vary little, being slightly below or above the neutral value. The lowest pH(H_2O) was measured in sample RDT2g, which also has a low pH(KCl) value, though a yet lower value was observed for sample PS1g. The corresponding value for the sample ZBB1g is below 6. The difference between the pH measured in H_2O and KCl is because active (functional) H^+ ions are measured in H_2O while adsorbed (exchangeable) H^+ ions are measured in KCl. The Eh values reported were calculated for goethite-bearing samples based on the pH-pĺ goethite stability diagram (Sánchez España et al., 2005). The lowest and highest Eh values were observed for the samples RDT4g and PS1g, respectively.

The Sodium Absorption Ratio values (SAR; from Iverson and Wali, 1992) are all based on total Na soil content and are all well below the threshold value of 12. As such, the soils studied may be treated as suitable for plant establishment. Acidity seems to be linked with SAR: the highest values of both parameters are seen in samples PS1g and ZBB1g. Most RDT samples show the lowest acidity values with the RDT2g sample being the only exception.

The samples studied differ strongly in terms of grain size distribution. They are largely non-homogeneous and of various grain sizes. The gravel+pebble fraction content varies from 41–89%; the sand fraction from 56–85%; and the silt fraction from 20–42%. There are similar variations as regards sub-fractions: 9–38% for the most coarse sand, 13–29% for 1.0–0.5 mm sand, 8–27% for 0.5–0.25 mm sand, 7–24% for the finest sand; and 4–23% for the finest silt. The most striking consistency concerns the clay fraction the content of which is very low or nil. The 0.1–0.05 and 0.05–0.02 mm silt sub-fractions also show relatively small variations, with ranges of 13–29, 0.25–10, and 1–15%. For all these ranges, and for the clay fraction range, the differences between the extreme values are <10%. Three samples, PS1g, RDT3g, and ZBB1g, are classified as gravel-rich clayey sands. Samples RD1g, RDT1g and RSH1g samples are gravel-clay deposits. The remaining samples, RDT2g and RDT4g, are distinctive in being gravel-rich sandy loams, the latter being pebble-rich.

The most gravel-rich samples, besides RSH1g, are RD1g and RDT1g. The sandiest sample is RDT3g followed by PS1g

Table 3

Results of PXRD-based Quantitative Phase Analysis using the Rietveld method

	PS1g	RD1g	RDT1g	RDT2g	RDT3g	RDT4g	RSH1g	ZBB1g
Quartz	38(1)[3]	21(2); 15[4]	26(1)	22(1)	24(1)	23(1)	19(2); 6	71(2)
Kaolinite	14(7)	8(1); 1	14(9)	11(8)	12(7)	11(9)	12(1); 4	8(6)
Illite	23(3)	25(4); 18	37(3)	38(3)	41(3)	40(3)	30(4); 10	2(2)
Chlorite group	3(3)	–	6(7)	4(5)	4(5)	4(4)	3(4); 1	–
Orthoclase	1(3)	2(3); 1	3(4)	2(3)	3(3)	2(4)	–	4(3)
Microcline	6(4)	2(5); 1	4(4)	3(3)	3(3)	2(3)	1(2); <1	3(3)
Albite	–	–	7(2)	6(5)	5(4)	6(5)	–	–
Anorthite	9(5)	15(2); 11	–	–	–	–	2(2); 1	0.5(4)
Anorthoclase	–	2(4); 1	–	–	–	–	–	–
Mullite	–	6(8); 4	–	–	–	–	21(2); 7	–
Sillimanite	–	–	–	–	–	–	1(2); <1	–
Indialite	–	4(1); 3	–	–	–	–	2(6); 1	–
Cordierite	–	1(2); 1	–	–	–	–	3(3); 1	–
Cristobalite	–	–	–	–	–	–	3(4); 1	–
Hematite	<1	7(8); 5	3(2)	3(2)	2(2)	3(2)	3(3); 1	–
Goethite	7(1)	4(6); 3	–	6(9)	6(9)	5(1)	–	–
Gypsum	1(1)	3(3); 2	–	2(2)	–	4(3)	–	–
Jarosite	–	–	–	2(2)	–		–	–
Sulphur	–	–	–	–	–	–	–	11(2)
Gls	–	29	–	–	–	–	66	–
R_{wp}[1]	9.25	5.47	9.64	7.43	7.92	8.83	5.12	10.79
GOF[2]	0.95	0.54	0.97	0.75	0.80	0.91	0.53	1.11

For glass-containing samples the original data obtained for the crystalline part is reported first; [1] – statistical parameter – residual weighted-pattern; [2] – statistical parameter – goodness of fit ([2]); [3] – wt.%; [4] – normalized content after amorphous (glass) phase calculation

and ZBB1g. Sample RDT4g is the least sandy but at the same time the richest in pebbles. As a loam, the latter sample is also the siltiest one, followed by RDT1g, RDT2g, RD1g, and RSH1g. The least silty sample is RDT3g. A large difference in silt content exists between two nearby samples. This is due either to variations in the fusion process occurring in the protolith and influencing the rock fabric, or to varying resistance to physicochemical weathering. Sample RSH1g is the most clayey, followed by PS1g, RD1g, RDT1g, and RDT2g. The latter four samples show very similar clay contents.

The 0.1–0.05 silt sub-fraction shows large variation. The highest content is in sample ZBB1g, followed by RSH1g and RDT4g, with RDT3g being the most depleted. The 0.05–0.02 sub-fraction, also characterized by wide variation, is most represented in the RDT4g and RSH1g samples, and the most depleted one being the RDT3g. The finest silt (0.02–0.002 sub-fraction) shows less variation, with similar contents most samples except for ZBB1g, which is significantly depleted. The coarsest sand (2.0–1.0 sub-fraction) has similar distribution, being most enriched in sample RDT3g, and least in RDT2g. The 1.0–0.5 sand sub-fraction has yet less variation, most enriched in sample RDT3g and least in RDT4g. The 0.5–0.25 sand sub-fraction is most abundant in sample ZBB1g, with a lower but more uniform content in most other samples (especially the RDT ones). The 0.25–0.10 mm fraction shows slightly greater variation among the sand sub-fractions, resembling that of the former sub-fraction.

DISCUSSION

Pyrometamorphic rocks are harder and less brittle than their protoliths. As such, they are more resistant to physical weathering, especially grinding. It was thus crucial for us to show that plant growth takes place not only at sites with visible humic or non-humic organic matter (e.g., PS1g, RDT3g, RSH1g), but also at nominally purely pyrometamorphic, i.e. inorganic, sites, (e.g., RD1g, RDT1g, RDT2g, RDT3g). Although at least some of the sites studied may be as old as a few decades (or more), no soil covers as thick as those reported by Novikova et al. (2015) for the Kuznetsk Basin pyrometamorphic outcrops were observed by us. Other structural and spatial characteristics of our soils also suggest their difference. For instance, weathered clinker areas are present in some of the BCWRs studied, but their thickness is significantly lower. Loamy soils of the Kuznetsk Basin are related to older sites. The RDT2g and RDT4g sites – the only soils attributed to loam – may, indeed, be relatively old, as no human reworking takes place there. However, the loamy nature of these two particular samples is more likely related to their vegetation and microbial activity. Furthermore, the steep slopes at the first site are a possible factor negatively influencing finer fraction enrichment, due to common deposition of large pyrometamorphic fragments originating from landslides.

ELEMENT ENRICHMENT AND METAL FIXATION

Enrichment in many elements, in particular in rare, trace, and precious elements including Ga, Co, Ni, In, and V, in both pyrometamorphic rocks and their minerals of the USCB BCWRs in seen in our initial studies. Coal-fire gases are the most important factor controlling element mobility and transport in the environment studied. Kruszewski et al. (2018) initially determined $Ca(OH)_2$, $Mg(OH)_2$, $Fe(OH)_2$, $Cu(OH)_2$, $Zn(OH)_2$, $Al(OH)_3$, SbH_3, Cu_2H_2 and other compounds in the USCB fire gas emanations.

Table 4

Results of the pedological analyzes of the soil samples as compared to examples of published data

Sample:	PS1g	RD1g	RDT1g	RDT2g	RDT3g	RDT4g	RSH1g	ZBB1g	geom. mean
pH_{H2O}	6.76	6.52	7.11	5.89	6.93	7.12	6.69	6.41	6.67
pH_{KCl}	4.59	6.44	6.83	5.42	6.39	6.80	6.10	5.76	6.00
Eh [mV][1]	0.18	0.06	–	0.12	0.00	–0.06	–	–	–
$CaCO_3$ [%][2]	<1	<1	3–5	<1	3–5	1–3	<1	<1	–
Exchangeable base cations EC [cmol(+)/kg]									
Ca_{EC}	3.76	9.56	16.36	29.56	22.76	**81.76**[3]	25.36	3.96	15.45
K_{EC}	0.04	0.09	0.12	**0.81**	0.13	0.30	0.14	0.01	0.11
Mg_{EC}	2.63	0.93	0.99	**5.18**	2.11	2.47	3.09	1.91	2.11
Na_{EC}	0.12	0.17	0.23	**1.36**	0.23	0.68	0.17	0.10	0.25
EA[4]	1.6	1.4	0.4	1.4	0.4	0.4	1.0	**2.2**	0.90
SAR[5]	0.7	0.4	0.5	0.5	0.4	0.3	0.4	**0.9**	0.5
Matrix content	high	very high	very high	high	high	high	very high	high	–
Colour	very dark gray 10YR 3/1	dark reddish brown 5YR 3/2	red 2.5YR 4/6[6] to dark reddish brown 2.5YR 3/3	dark reddish brown 2.5YR 3/3 to red 2.5YR 5/6[7]	light reddish brown 5YR 6/4, reddish brown 5YR 4/3, very dark gray 5YR 3/1	very dark gray 10YR 3/1	black 10YR 2/1	black 2.5/N GLEY 1	
Particle size (mm) distribution (%)									
Skeleton >2 mm	53	70	61	49	48	54	**89**	41	57
Fine earth <2 mm	47	30	39	51	53	46	11	**59**	38
sand	78	66	60	63	**85**	58	56	77	67
silt	20	32	**38**	34	14	42	37	20	28
clay	2	2	2	3	1	0	**7**	3	2
Sand sub-fractions [%]									
2.0–1.0[8]	26	26	22	18	**38**	17	27	9	21
1.0–0.5	23	16	14	14	**29**	13	14	18	17
0.5–0.25	17	12	12	14	15	14	8	**27**	14
0.25–0.1	12	12	13	17	3	15	7	**24**	11
Silt sub-fractions [%]									
0.1–0.05[8]	1	3	4	2	0.25	9	9	**10**	3
0.05–0.02	7	13	14	**15**	1	10	8	6	7
0.02–0.002	12	16	20	17	13	**23**	20	4	14
Lithology	grcs[9]	gcf	gcf	grsl	grcs	gprsl	gcf	grcs	

[1] – calculated from p which values were derived from a pH-p goethite stability diagram (Sánchez España et al., 2005); [2] – tentative content, by HCl method; [3] – highest observed values are given in bold; [4] – exchangeable acidity [cmol(+)/kg]; [5] – sodium absorption ratio (Iverson and Wali, 1992); [6] – large fragments; [7] – rarely (locally); [8] – in [mm]; [9] – grcs – gravel-rich clayey sand, gcf – gravel-clay formation, grsl – gravel-rich sandy loam, gprsl – gravel- and pebble-rich sandy loam

The soils studied show enrichment in many elements, including many metals, but the concentrations determined are not high. The most persistently enriched trace elements are Sb, As, and Pb. Other, less commonly enriched elements are Al, Cu, and Ba. Enrichment factors for these elements as compared to soil means (Kabata-Pendias and Pendias, 1989) are 7–14; 2–4; 2–4; <2; <5; and <3, respectively. Some other elements show single-sample anomalies. Mean contents of all the main elements in the soil samples studied are larger than those determined for both local coals and shales. This is especially true for the following trace elements: As, Ba, Co, Cr, Cu, La, Mn, Nb, Ni, Pb, Sb, Sc, Sr, Th and Y. As compared to average PM rock contents (as derived from Kruszewski, 2018), the soils are clearly enriched in Sb, Zr, and also As, Cu, Pb, Sn, and Zn. They also show moderate to slight enrichment in Ba, Be, Nb, Ni, and Th. The mean elemental composition of the soils was also compared to the Coal Clarke (CC, that is, mean) values of Ketris and Yudovich (2009). Similarities include P, Ti, and Ag, with significantly larger or larger soil values for most other elements. As compared to average concentrations in soils (from

Kabata-Pendias and Pendias, 1989 for TEs; from Mocek, 2015, for major elements), our samples show high enrichment in Fe, Pb, and Zn, and moderate enrichment in Ca, Mg, S; As, Ba, Be, Bi, Cu, Nb, Ni, Sn and Th. Depletion in this case largely concerns K.

Samples most enriched in elements, in general, are RSH1g, RD1g, and RDT3g – all being of pyrometamorphic substrate type. The first sample is geochemically involved with maximum observed concentrations of Cr, Ba, Ni, Sb, and Zn; and enriched in As, Co, V, and somewhat in Zr. The second sample, interestingly, shows the highest enrichment in the major elements Fe, Mg, P, Na. It is also clearly enriched in Ca and Al and has elevated As, Ba, Be, Co, Cu, Nb, Sc, Th, V, Y, and Zr levels. Sample RDT3g has the largest amounts determined of Al, K, La and Th, and is also enriched in Ca, Fe, Mg, Ti, Sc, Y, Zr. Sample RDT4g shows the highest levels of Ca, Mn and W, and enrichment in Fe and S. Samples RDT2g and RDT1g are characterized by elevated Pb, K, Al and Fe contents. Sample PS1g only shows some enrichment in Cr and Th. Sample ZBB1g is the most S-rich and has elevated Na and Ca contents being, otherwise, the most geochemically depleted one. Mineralogy explains some of these variations, e.g., hematite correlates with high Fe in sample RD1g; elevated gypsum with high Ca and elevated S in RDT4g; goethite with elevated Fe in RDT3g or RDT2g. Four same-heap soils show different enrichment images; this is likely not just due to different mineralogy, but most likely also the distinct chemistry of the pore solutions. Relative depletion in sample RDT1g may also be caused by higher amounts of elements transported, as the slope is the steepest and the rhizosphere is virtually absent there.

From the sozological point of view, the soils studied are far from posing a toxic threat to the surrounding environments. The TE concentrations measured do not exceed the maximum threshold values reported by both Mocek (2015) and the Polish Environment Ministry Ordinance of 05.09.2016. Our results are, however, different from those reported for Ruhr CWR soils (Meuser, 2013): only Ni shows values <80 ppm; all USCB BCWR soils exhibit Pb concentrations larger than 30 ppm, while most also having Cu >50 ppm and Zn >70 ppm. Even mean concentrations of these 3 elements are above the thresholds reported by Meuser (2013). Moreover, all of the observed Cu, Pb, Ni, and Zn values are much higher than those for the Tula area CWR soils and higher than the Chinese BCWR data of Jiang et al. (2014). Increased Zn, Pb and Cd contents are present in the Sosnowiec surface soils studied by Cabala et al. (2006).

All the samples studied seem to be sufficient in terms of metallic macronutrient content. Al toxicity, related to the Al_w parameter, was not observed, presumably due to relatively high pH.

CHNS AND PHOSPHORUS CHARACTERISTICS

As the solid carbonate content in our samples is very low or nil, most of the C measured is in its organic form. Although no macroscopically distinguishable coal fragments were observed in the samples, a small amount of shale-hosted coal is possible in sample PS1g. Sample RSH1g has the highest C content, followed by ZBB1g and RDT4g. In the first and last of these, humic substance was seen *in situ*. In just one sample, ZBB1g, most of the carbon is contained in thermally altered coal-derived organic matter. Although humus was also observed in Pszów, the plant coverage and heap age are clearly different than in the Ruda Śląska location. Sample RDT1g, with the lowest C content, did not show any macroscopic humic substance *in situ*.

The C content determined is much higher than that reported by Upadhyay et al. (2016) for an Indian CWR, with a maximum value of 0.65 %. Even less total organic carbon, 0.28 %, was reported for soil of another Indian CWR by Tripathi et al. (2012). Their total N and P contents are also much lower, at 0.045 and 0.009%, respectively. It is, however, difficult to address their data in more detail due to the remediation-related character of their work. The C content measured for the USCB BCWR soils is comparable to that reported by Garrison et al., (2016) for the Kentucky coal-fire sites, ranging from 3.18–14.32%, the latter value still being lower than that of sample ZBB1g.

The samples studied may be divided into two groups as regards hydrogen content. Samples with >1 wt.% H include the humic-rich RSH1g (most H-rich) and RDT4g, and the organic-pyrolysate-rich ZBB1g. The other group begins with RDT3g, followed by RDT2g with OH-containing jarosite and H_2O-bearing gypsum, sample PS1g, and samples RDT1g and RD1g which are typically pyrometamorphic, and so low-organic.

Sample ZBB1g sample is the only one with >1 wt.% N, undoubtedly related to the N content in thermally changed organic matter. Indeed, coal-fire organic pyrolysates contain heterocyclic N compounds. Some nitrogen (and chlorine) may also be contained in the otherwise ephemeral salammoniac – a product of coal-fire gas condensation – but also in related solutions. As noted in the Introduction, the fire gases themselves carry a number of N-rich gases. Moreover, gas condensation is responsible for the presence of elemental sulphur in sample ZBB1g. Thus, the fires gases influence the soil nitrogen, sulphur, and chlorine budget but may also introduce some metals, semimetals, and other non-metals, as suggested by Querol et al. (2011). The last group of compounds comprises AsH_3, HF and SiF_4 (Kruszewski et al., 2018, 2019). Most samples showed an average N content, though those for ZBB1g and RSH1g are comparable to the highest values reported for abandoned USA coal mine soils by Iverson and Wali (1992).

All our samples show C/N values (10–46 range) close to the 9–42 range reported for relatively young post-mining USA soils by Iverson and Wali (1992). Samples arranged in descending order of the C/N ratio are RD1g, RDT4g, RSH1g, RDT3g, and PS1g. Samples with C/N 15 are RDT1g, RDT2g, and ZBB1g. The RDT2g and RDT4g loamy samples, discussed above in the context of the Novikova et al. (2015) data, seem to be grouped differently in this case. It is difficult to compare our C/N ratios to the USA ones as a heterogeneous genetic character of the organic matter is suspected in our samples. The Sample ZBB1g is extreme in this respect. Such incongruity is related to the variable character of the protolith, plant activity, type of soil organic matter, and particular N species distribution.

Four groups of samples may be distinguished as regards S content. The native sulphur-bearing sample ZBB1g comprises the first group, with >4 wt.%. The most gypsum-rich sample RDT4g constitutes the next group. The third group, with S content in the >1–0.5 wt.% range, includes RDT2g (gypsum- and jarosite-bearing) and RDT1g with gypsum only. Most samples belong to the fourth group, at <0.5 wt.% S, with RSH1g being the most depleted. Its S is contained exclusively in the organic phase, as this sample bears no gypsum presumably either due to protolith geochemical character, pyrometamorphism temperature, or biodegradation. Lacking gypsum at this site seems to be correlated with high Ca_{EC} concentration, possibly allowed by slightly acidic soil pH. The sulphur content measured by ICP shows a clear positive correlation trend with the sulphur content obtained by CHNS ($r^2 = 0.99$). Even the lowest of our measured S values are >10 times larger than the highest value reported for the Centralia soils by Tobin-Janzen et al. (2005).

The phosphorus content in most of our samples is much higher than that reported by Meuser (2013) to be insufficient for

vegetation (i.e., 200 ppm). This is not true only for the generally chemically impoverished ZBB1g sample, with exactly the threshold content. Also, our soils bear much higher P content than the highest amounts reported by Iverson and Wali (1992) for both non-remediated and reclaimed post-coal-mining soils of the USA.

SOIL MINERALOGY

The mineralogical composition of the soils covering typical pyrometamorphic substrates is not an exact reflection of substrate mineralogy. Although quartz, as a relic phase, and minor hematite, indialite, mullite, and anorthite are present, the soils studied are enriched in clay minerals which are either largely destroyed or completely absent in the original pyrometamorphic rocks. Samples PS1g and ZBB1g are the only ones where the clay minerals – or at least a portion of them – are derived from already clay-containing (i.e, with illite, kaolinite, and minor chlorite-group species) black shales. The remaining, rather substantial fraction of the clay minerals is supposedly a product of pedogenic weathering of clinkers and other, minor, rocks. Goethite and to some extent jarosite are further pedogenic components of the soils. Querol et al. (2011) suggested gypsum formation in Chinese BCWR soils as a result of an interaction between ascending fumarolic SO_2 and H_2S and Ca-rich soil minerals such as calcite. However, gypsum is also a common late-stage pyrometamorphic mineral.

Soil pH is not a determinative factor for goethite occurrence. This species is stable at a wide range of pH, assuming SO_4^{2-} content <1000 μg/mL (Hammarstrom et al., 2005). Depending on Eh, goethite may exist at pH as low as 2 or close to neutral (Sánchez España et al., 2005). The abundance of gypsum in the samples studied is likely related to the intensity of local fumarolic activity. Indeed, sample RDT4g was collected from the vicinity of a crack in which gypsum was observed. The crack itself represents the apical part of an active sulphate-rich fumarolic zone. Gypsum-bearing fumaroles were also once noticed in the Pszów heap, at the same horizon as the soil sample collection site. In other sites the source of gypsum seems to be weathering, and may reflect more carbonate rocks in the pyrometamorphic protolith.

PEDOGENIC PARAMETERS

Enrichment of the soils studied in sand is consistent with the observations of Atanassova et al. (2018). The sand fraction and the 0.05–0.002 silt sub-fraction in the Czerwionka BCWR soils are, on average, in the 22–25% and 68–70% ranges, thus being similar to those in our samples. However the clay content is higher, with values commonly ~7% and reaching up to ~12% (Zając and Zarzycki, 2013). Sandy clay loam and sandy loam are soil textures found also by Upadhyay et al. (2016) at the Indian CWR sites. However, their soils are much more clay-enriched, a feature most likely related to a more shaly than clinkery character of the waste. The USCB BCWR soils also differ from post-mining USA soils studied by Iverson and Wali (1992), in terms of silt and, especially, clay abundance. A high variability of grain size distribution in the soil samples studied reflects both different collection niches (or sub-environments) and chaotic waste deposition within the particular BCWRs. However, the high content of largest size fractions in the RSH1g and RD1g samples seems to follow their higher-temperature history, linked with the occurrence of high-temperature minerals.

Although the RDT samples were collected from genetically similar pyrometamorphic bodies, sample RDT2g sample is extraordinary in some aspects. Its lithology is unique with the lowest pH(H_2O) among the samples studied. This sample is also the most enriched in exchangeable K, Mg, and Na. The remaining RDT (and other heap) sample lack jarosite. These characteristics are most likely related to an extensive rhizosphere at the collection spot. Although the rhizosphere is much less pronounced at site RDT1g, the C-level rocks located there are clearly comminuted.

Sample RSH1g also unique in terms of its lithology. Paradoxically, it has the highest content of both the coarsest and the finest fractions. This may be linked to the unusual nature of both collection sites – a breccia block separated from the parent heap body – and strong substrate reworking by the local plants. This particular sample was collected both underneath moss cover and between the roots of a large tree, within a very small space. Indeed, bioactivity may be responsible for the highest, though still small, portion of clay fraction in sample RSH1g. Plant activity is also likely responsible for divergence in silt content in sample RDT3g as compared to other RDT soils. Although the clay fraction is minor in all samples studied, it is widely present in the most frequent component of the BCWRs, these being quartz-illite-kaolinite black shales.

The most pedogenically aberrant sample is undoubtedly ZBB1g. This reflects the sub-environmental niche of its collection point as the only active and organic-pyrolysate-rich of the soil collection spots in this study. Such a location dictates unique mineralogical properties (in particular, the presence of elemental sulphur) and its general barren character in terms of both nutrient contents and plant coverage. The hydrocarbon-rich and other simple-organics-bearing matter does not make a good substrate for plant growth. Although such types of organics may be altered by some fungi (e.g., Gusse et al., 2006), no such white rot fungi were observed *in situ*.

The pH values observed in our soils vary over a 1.23 range for water-measured pH and 2.24 for the KCl-measured one. Also, the mean pH(H_2O) value of 6.67 is close to the values measured in at least half of the samples. A higher pH value span of 2.7 characterizes the post-mining soils of Arefieva et al. (2019), while that for the Pernik remediated CWR (Meuser, 2013) is even higher (>3.7). No pH values as low as 3.77, as for some post-mining soils studied by Iverson and Wali (1992), nor the even lower values of the 1.8–2.5 range of the Tula area (Meuser, 2013), were observed by us. Also the Martinez and Ressler (2001) and Tobin-Janzen et al. (2005) data for the Centralia soils reveals more acidic (pH of 3.5–6 in the first and 4.1–5.8 in the second case) conditions. The pH values reported for the Czerwionka BCWR by Zając and Zarzycki (2013), of average 4.06–4.83 (H_2O basis) and 3.54–4.00 (KCl basis) ranges, are obviously lower than our determinations due to the specific location of their study: a pile with intense sulphate mineralization processes in its core. Values as high as 7.7 on average, as observed for the Chinese CWR by Jiang et al. (2014), were not seen in any of our samples. Our pH range is more similar to that reported by Upadhyay et al. (2016), being 5.39–6.29, even though their studied heap does not seem to be on fire.

The average CEC values reported for the Czerwionka BCWR soils (Zając and Zarzycki, 2013) are in the 4.18–5.21 range, with a 4.37–5.72 range representing maximum values. According to the classification of Lityński (1971), our EC values show the soil studied to be of high to very high sorptive capacity. This may be because, according to Atanassova et al. (2018), non-vegetated soils should show higher EC values. Our soils are, indeed, relatively low in vegetation cover.

ELEMENT-MINERAL CORRELATIONS

As reported (e.g., Egozcue and Pawlowsky-Glahn, 2005; Filzmoser et al., 2010; Buccianti et al., 2014; Kynčlová et al.,

2017), simple bivariate graphs have limited interpretability due to the closed character of the data used (constant sum constraint). The authors listed above suggest a log ratio approach, which we used. These are still insufficient to allow correct data transformation in the case of Pearson-type juxtaposition for elements contained in the same data group. As such, we cannot report reliable r^2 values for the potential trends we observed for intra-elemental (i.e., intra-ICP) graphs. The authors listed suggest multidimensional statistics as the correct tool for geochemical data. However, we cannot successfully apply such an approach due to the small number of samples, in this pilot study.

Element-mineral correlations are listed in Appendix 2. The highest r^2 values are obtained for goethite, always negatively correlated with some elements including Na, Sr, P, Co, and As. Goethite is a known As (e.g., Amstaetter et al., 2009; Mamindy-Pajany et al., 2009) and Co (e.g., Ugwu and Sherman, 2017) environmental sink. It is also capable of adsorbing phosphate ions (e.g., Parfitt and Atkinson, 1976) and Na (e.g., Schulthess and Ndu, 2017) but the latter association may also be pH-related. However, these authors also modelled and showed Cl^- ion sorption by goethite. The USCB coal deposits are associated with juvenile brines (e.g., Pałys 1966), expected to be present in the heap wastes as pore waters. This may be reflected in rich salammoniac and other chlorides in the fumarolic crusts and positive determination of various Br- and I-bearing gaseous compounds and minerals in the USCB BCWRs (e.g., Kruszewski et al., 2018). As such, goethite may not only represent a pedogenic indicator but also a local, potential adsorptive salinity factor. Its sorption capabilities may also govern variations observed in element enrichment patterns seen in some RDT samples. This may also be true of elevated REEs in sample RDT3g.

Plagioclase and illite show the largest number of correlations with elements potentially contained in them. Plagioclase is positively correlated with mainly Na, followed by Mg, Al, Fe, K, Cu, Th, and Y. Additionally, our experimental and non-experimental pyrometamorphic data (e.g., Kruszewski, 2013a) shows pyrometamorphic plagioclase being capable of incorporating large amounts of Mg and Fe. A number of pyrometamorphic minerals are known to carry various elements nominally not entering their sites – a phenomenon related to their rapid crystallization under high thermal gradients (e.g., Kruszewski, 2013b). Strong negative correlation of plagioclase with N and less pronounced correlation with H are suggestive of NH_4^+ substitution. Indeed, Bindeman and Davis (2000) reported this cation as capable of entering the plagioclase structure. However, due to the relatively large difference between Ca^{2+} and NH_4 radii, this phenomenon seems negligible if not affected by a steep thermal gradient. Also, although plagioclase is nominally anhydrous, traces of water and OH^- may be present (e.g., Ruefer et al., 2018). Plagioclase, however, supplies little or no N and H.

As a clay mineral, illite is known to sorb heavy metals in its interlayer space (e.g., Uddin, 2017). Indeed, illite-bearing clays have been suggested for soil remediation (e.g., Ou et al., 2018). In our samples, illite is obviously strongly positively correlated with K and Al and, to some extent, with Mg, Fe, and Ti. It is also known to immobilize Nb, Sc, Mn, and to a lesser degree also V, Th, Co, Y, Ni, Cr, and possibly Sr. A strong negative Sb-illite correlation is questionable.

A number of elements show negative correlation with quartz – a phenomenon especially strong in the case of Zn. The same is true for Sb, Ba, and to some extent for Cr, Ni, P, Sr, Co, and Nb. We suspect the only reasonable cause for this correlation is quartz-clay and quartz-plagioclase concentration competition. Chlorite-group species show strong positive correlation with Na, while the remaining three correlations with H, N, and Sb are negative. Such Na behaviour is unexpected. We thus, again, suspect that chlorite-related correlations represent mineral content issues only. Sodium is, again, strongly positively correlated with hematite. The contemporaneous strong negative correlation in the Na-goethite system suggests that Na is somehow related to goethite occurrence. A possible clue is given by Murray et al. (2009) who report hydrothermal goethite-to-hematite transformation, at 200–250°C, in sodium aluminate solution. However, their process takes place at slightly elevated pressure. Also, we do not suspect a reaction between hematite and goethite to act in such direction in the environment studied. As in the case of quartz, zinc is negatively correlated with hematite. Since no evident positive correlations of Zn with minerals constituting the soil samples were found, this element could possibly be present in soil solution and/or sorption complex. K-feldspar and gypsum are minerals rarely correlated with elemental sample composition. Negative correlations in the first case concern Ca and Na, probably simply representing the affinity of Ca and Na to non-alkaline-feldspar species. Besides obvious strong correlation with S, gypsum is also, interestingly, positively correlated with C. No evident correlations of any element with kaolinite were noticed, presumably as that mineral lacks expandable layers. Relatively r^2-high correlations that could likely pass the Mann-Whitney test when a larger dataset is used include positive S-gypsum and negative Sb-gypsum, Fe-goethite, and V-goethite. Most of them seem also geochemically reliable.

INTRA-ELEMENT CORRELATIONS

Intra-element correlations based on ICP and CHNS datasets comparison are shown in Appendix 3. The following trends, all negative, were observed: Al-N and Al-S; Ba-S; Co-N; Cr-S and Cr-N; Cu-N; Fe-N; K-S and K-N; La-N and La-S; Mg-N; Mn-N; Na-H and Na-N; Nb-N and Nb-S; Ni-N; Sc-N and Sc-S; Sr-N; Th-N and Th-S; Ti-N and Ti-S; V-N and V-S; Y-N; Zr-N and Zr-S. These pairs are ordered according to corresponding theoretical r^2 values. The number of samples is very low due to the pilot character of our study, thus these potential trends are still of limited significance.

The negative K-S correlation suggests K not entering sulphate compounds at the surface, soil-bearing environment of the BCWRs. The negative K-N correlation appears to be related to the well-known K-NH_4 diadochy that is commonly observed in both ammonium- and potassium-dominant exhalative and supergene (and thus surface or subsurface) water-soluble sulphate minerals of the BCWRs (e.g., Kruszewski, 2013a; Kruszewski et al., 2018). It is debatable whether these two negative trends involving K are linked to the use of K^+ and not SO_4^{2-} and NH_4 by the local plants.

Negative correlations of some elements with S and N may suggest some of these elements being brought from their initial sinks in the form of sulphates and nitrates. This is interesting from the sozological and also industrial point of view due to the observed, potential correlations of Sc, Ti, V, Zr, La, Th (the well-known HFSE group), Cr, vanadium (other transition metals) and Al and K, with both S and N. A similar process may concern the N-correlated elements Cu, Co, Fe, Mg, Mn, Ni, Sr, and Y. As most of these elements are found together in many geological situations (e.g., weathering), their nitrogen correlation trends seem to be reliable. The Ba-S correlation is, in turn, consistent with the relatively common observation of baryte, $BaSO_4$, as micro-inclusions in various pyrometamorphic rocks of the USCB BCWR This is another important sozological factor that makes enriched, toxic barium immobilized in BCWR soils as its highly insoluble sulphate form.

Table 5

Correlation of elements with fractions (both log ratio-transformed), as imaged by Pearson r^2 values, element systems with r^2 <0.40 are not listed

	>2 mm	sand (total)	sand (2–1 mm)	sand (0.5–0.25 mm)	sand (0.25–0.1 mm)	silt (0.02–0.002 mm)
Al			**.75**			.66
As				.63[1]		
Ba[2]			.62	**.80**		.53
Ca						.51
Ca^{2+} [4]						.54
Cu			.50	.61		**.79**
Co	.51			**.78**		**.92**
Cr			.64	**.82**		**.81**
Fe			.53	.59		**.88**
K			.68			.69
K^+ [6]						.66
La			**.81**		.55	
Mg			.60	.51		**.81**
Mn				.58		**.90**
Nb			.69	.66		**.79**
Ni			.55	**.83**		**.89**
P	.51	.42		**.75**		**.85**
Pb				.59		.66
Sb	**.78**[3]			**.91**		
Sc				.59		.69
Sr				.68		**.75**
Th			**.87**		.52	
Ti			.70	.64		**.77**
V			.57	.74		**.84**
Y			.67			.57
Zn	.71[5]	.45		**.94**		.63
Zr			**.84**	.52		.51
N	.50					

[1] – negative trends are underlined and r^2 values 0.75 are given in bold; [2] – somewhat negatively correlated with <2 mm fraction content (r^2 = 0.49); [3] – negatively correlated with <2 mm fraction content (r^2 = 0.88); [4] – somewhat positively correlated with <2 mm fraction content (r^2 = 0.47); [5] – negatively correlated with <2 mm fraction content (r^2 = 0.69); [6] – exchangeable basic cations

The exchange capacity (EC) of K^+ and Ca^{2+} is slightly positively correlated with their total forms. Such dependencies were not found in the case of Na and Mg, possibly due to their stronger adsorption. The exchangeable acidity (EA) parameter was also not found to be correlated with any elemental data.

ELEMENT/MINERAL – pH RELATION

Correlations in the given system are listed in Appendix 4. They are rare and associated with the main elements of the sorption complex (Na_{EC}, K_{EC}, and Mg_{EC}) that are to a degree polynomially correlated with pH(H_2O) and – in the case of Na_{EC} – also with pH(KCl). No correlation of Ca_{EC} with any pH measured was established. This element seems to be generally linearly correlated with pH(KCl). Gypsum is the only mineral for which a strong (r^2 = 0.80), positive correlation was observed. This is suggestive of relatively high SO_4^{2-} activity in particular soil solutions assuming conditions unchanged since gypsum crystallization. Nevertheless, our observations do not follow numerous element-pH correlations observed for post-mining soils by Arefieva et al. (2019). The pH values measured by Tobin-Janzen et al. (2005) in the Centralia fire soils are in the 4.1–5.8 range, NH_4 contents in the 0.43–76 ppm range, NO_3 in the 0.45–103 ppm range, and total S as high as 159 ppm on average. Local enrichment of NH_4 and NO_3 in the boreholes analysed was interpreted as a proof of nitrifying bacteria activity.

ELEMENT – GRAIN SIZE RELATION

Correlations between elemental and grain size composition of the soil samples studied are given in Table 5. Correlation trends were shown for 27 elements. As many as 23 elements, excluding As, La, Sb, Th, and N, were found associated with the finest silt sub-fraction. All these correlations are positive and the strongest ones concern Co, Mn, Ni, Fe, P, V, Mg, Cu, Nb, Ti and Sr (r^2 >0.80). The following, slightly less correlated, elements are Sc, Al, K, Pb, Zn, Y, Ca, Ba, and Zr. The first group mainly includes *d*-block transition siderophile ("iron loving") elements and some HFSE elements and to a large extent corresponds with a group of elements correlated with illite. This demonstrates illite as the volumetrically most important trace-element carrier in the soils studied.

As many as 19 elements show negative correlation with the 0.5–0.25 mm sand sub-fraction, with r^2 0.80 for Zn, Sb, Ni, Cr, and Ba. Many of these have positive finest silt correlation counterparts. This is not true for Sb and As, though these were found only in samples 6 and 7, which is expected to affect the entire correlation behaviour of these elements. More importantly, 15 elements were found to be positively correlated with the coarsest sand sub-fraction. They include Th, Zr, La – HFSE group representatives – and Al (r^2 0.75); and Ti, Nb, K, Y, Cr, Ba, Mg, V, Ni and Cu. Similar behaviour of Th, Zr, La and other HFSE elements seems to support the correlation trends shown.

A link between elemental composition and grain size distribution does not seem to be plausible. Almost none of the elements analysed was found correlated with any of the grain size fractions. Only Sb and Zn seem to be positively correlated with gravel/pebble fractions. While no explanation for such Zn behaviour may be found currently, Sb behaviour seems to be similar to that discussed above.

PLANT HABITAT CONDITIONS IN THE BCWR

The soils studied are neither very acidic, nor basic. This suggests good conditions for plant development. Soil acidity related to either coal mining waste decomposition or depletion in larger grain sizes, as addressed by Meuser (2013) or Upadhyay et al. (2016), is not the case in the USCB soils studied. Toxic Al is also not the case here, most likely lessened by the action of fires as also observed by de Rouw (1994).

CONCLUSIONS

By studying 8 soil samples from various BCWRs, collected in both pyrometamorphic and non-pyrometamorphic niches, we can conclude that:

1. Initial soils may develop in sites with both thermally or exhalatively transformed substrates; the former is pyrometamorphic while the second is thermal-organic in nature;
2. Organic matter in such soils is more complex than in “normal” soils due to the possible addition of thermally changed organic matter;
3. There is a large range in grain size distribution, even in soils collected on the same body;
4. Most of the soils studied have some plant cover developed; the single organic-rich soil studied lacks this, but some plants were found in its direct vicinity;
5. Element enrichment, in particular of the potentially toxic elements, in the soils is distinct but not extreme;
6. The most commonly enriched trace elements are Sb, As, Pb, with less pronounced enrichment of Ba and Cu; this enrichment is at least partially related to gaseous element transport;
7. Most elements seem to be enriched in the finest silt fraction, where illite appears to be the main trace element carrier;
8. A strong goethite-sodium correlation seems to represent a Na^+ and Cl^- adsorptive relation. This may make the goethite a potential, though local, salinity factor; its sorption capabilities may govern some other elemental characteristics;
9. Higher mineral crystallization temperatures in samples RSH1g and ZBB1g not only results in different mineralogical compositions but also causes the greatest elemental enrichment.
10. The relatively invariable pH, non-extreme heavy element contents, lacking Al_w, and average nutrient contents generally fulfil vegetation needs.

Acknowledgements. This work was financially supported by the statutory funds of the Ministry of Higher Education and Science for the Institute of Geological Sciences, Polish Academy of Sciences (for 2019).

REFERENCES

Abramowicz, A., Rahmonov, O., Chybiorz, R., Ciesielczuk, J., 2021. Vegetation as an indicator of underground smoldering fire on coal-waste dumps. Fire Safety Journal, **121**: 10.1016/j.firesaf.2021.103287

Amstaetter, K., Borch, T., Larese-Casanova, P., Kappler, A., 2009. Redox Transformation of Arsenic by Fe(II)-Activated Goethite (-FeOOH). Environmental Science and Technology, **44**: 102–108.

Arefieva, O., Nazarkina, A.V., Gruschakova, N.V., Skurichina, J.E., Kolycheva, B., 2019. Impact of mine waters on chemical composition of soil in the Partizansk Coal Basin, Russia. International Soil and Water Conservation Research, **7**: 57–63.

Atanassova, I.D., Benkova, M.G., Simeonova, T.R., Nenova, L.G., Banov, M.D., Doerr, S.H., Rousseva, S.S., 2018. Heavy metal mobility and PAHs extractability relationships with soil hydrophobicity in coal ash reclaimed technogenic soils (Technosols). Global Symposium on Soil Pollution, 2–4 May 2018, Fao, Rome, Italy. Proceedings , Food and Agriculture Organization of the United Nations: 209–218. Food and Agriculture Organization of the United Nations.

Awoyemi, O.M., Dzantor, E.K., 2017. Fate and impacts of priority pollutant metals in coal fly ash – soil – switchgrass plant mesocosms. Coal Combustion and Gasification Products, **9**: 42–51.

Bhatla, S.C., Lal, M.A., 2018. Plant Physiology, Development and Metabolism. Springer.

Bindeman, I.N., Davis, A.M., 2000. Trace element partitioning between plagioclase and melt: investigation of dopant influence on partition behaviour. Geochimica et Cosmochimica Acta, **64**: 2863–2878.

Buccianti, A., Egozcue, J.J., Pawlowsky-Glahn, V., 2014. Variation diagrams to statistically model the behavior of geochemical variables: theory an applications. Journal of Hydrology, **519**: 988–998.

Cabala, J., Idziak, A.F., Szymala, A., 2006. Physicochemical and geophysical investigation of soils from former coal mining terrains in southern Poland. In: Proceedings of the 15th International Symposium on Mine Planning and Equipment Selection, Torino (eds. M. Cardu, R. Ciccu, E. Lovera and E. Michelotti): 534–548.

Drenda, J., Różański, Z., Słota, K., Wrona, P., 2007. Zagrożenie pożarowe na zwałowiskach odpadów powęglowych (in Polish). Górnictwo i Geoinżynieria, **31**: 149–157.

de Rouw, A., 1994. Effect of fire on soil, rice, weeds and forest regrowth in a rain forest zaone (Côte d'Ivoire). Catena, **22**: 133–152.

Egozcue, J.J., Pawlowsky-Glahn, V., 2005. Groups of parts and their balances in compositional data analysis. Mathematical Geology, **37**: 795–828.

Filzmoser, P., Hron, K., Reimann, C., 2010. The bivariate statistical analysis of environmental (compositional) data. STOTEN, **19**: 4230–4238.

Garrison, T., Hower, J.C., Fryar, A.E., D'Angelo, E., 2016. Water and soil quality at two eastern-Kentucky (USA) coal fires. Environmental Earth Sciences, **75**: 574–587.

Gusse, A.C., Miller, P.D., Volk, T.J., 2006. White-rot fungi demonstrate first biodegradation of phenolic resin. Environmental Science and Technology, **40**: 4196–4199.

Hammarstrom, J.M., Seal II, R.R., Meier, A.L., Kornfeld, J.M., 2005. Secondary sulfate minerals associated with acid drainage in the eastern US: recycling of metals and acidity in surficial environments. Chemical Geology, **215**: 407–431.

Hänsch R., Mendel, R.R., 2009. Physiological functions of mineral micronutrients (Cu, Zn, Mn, Fe, Ni, Mo, B, Cl). Current Opinion in Plant Biology, **12**: 259–266.

Iverson, L.R., Wali, M.K., 1992. Grassland rehabilitation after coal and mineral extraction in the Western United States and Canada. Ecosystem Rehabilitation, **2**: Ecosystem analysis and synthesis. The Hague, Netherlands, SPB Academic Publishing: 85–129.

Jiang, X., Lu, W.X., Zhao, H.Q., Yang, C., Yang, Z.P, 2014. Potential ecological risk assessment and prediction of soil heavy-metal pollution around coal gangue dump. Natural Hazards and Earth System Sciences, **14**: 1599–1610.

Juda-Rezler, K., Kowalczyk, D., 2013. Size distribution and trace elements contents of coal fly ash from pulverized boilers. Polish Journal of Environmental Studies, **22**: 25–40.

Kabała, C., Drewnik, M., Jankowski, M., Marzec, M., Mendyk, Ł., 2019. Przewodnik terenowy do opisu gleb (in Polish). Polskie Towarzystwo Gleboznawcze. Warszawa.

Kabata-Pendias, A., Pendias, H., 1989. Mikroelementy w pochvakh i rasteniyakh (in Russian). Mir, Moscow, Russia.

Karczewska, A., Kabała, C., 2019. Metodyka analiz laboratoryjnych gleb i roślin (in Polish). 8rd editon. Akademia Rolnicza, Wrocław.

Ketris, M.P., Yudovich, Ya. E., 2009. Estimations of clarkes for carbonaceous biolithes: world averages for trace element contents in black shales and coals. International Journal of Coal Geology, **78**: 135–148.

Kim, A.G., 2007. Greenhouse gases generated in underground coal-mine fires. GSA Reviews in Engineering Geology, **18**: 1–13.

Klatka, S.T., Malec, M., Ryczek, M., 2019. Analysis of spatial variability of selected soil properties in the hard coal post-mining area. Journal of Ecological Engineering, **20**: 185–193.

Knicker, H., 2007. How does fire affect the nature and stability of soil organic nitrogen and carbon? A review. Biogeochemistry, **85**: 91–118.

Kokowska-Pawłowska, M., 2015. Petrographic and mineral variability of the rocks accompanying selected coal seams of the Poruba beds and their influence of the trace elements content. Mineral Resources Management, **31**: 73–92.

Kruszewski, Ł., 2013a. Supergene sulphate minerals from the burning coal mining dumps in the Upper Silesian Coal Basin, South Poland. International Journal of Coal Geology, **105**: 91–109.

Kruszewski, Ł., 2013b. Synthesis of diverse chemically and structurally unique substances from coal-mining heap waste during experiments in diffraction-coupled thermal chamber. Science for Industry: Necessity is the mother of invention. 2nd Networking event in the field of modern techniques in geosystem exploration, conference, Warsaw, Poland.

Kruszewski, Ł., 2018. Geochemical Behavior of Trace Elements in the Upper and Lower Silesian Basin Coal-Fire Gob Piles of Poland. Chapter 19. In: Coal and Peat Fires: A Global Perspective, **5** – "Case Studies – Advances in Field and Laboratory Research": 407–449.

Kruszewski, Ł., Fabiańska, M., Ciesielczuk, J., Segit, T., 2017. Coal fires – titan – interstellar medium – life: what do they have in common? Potential gaseous bio-precursors in burning mining heaps. Life Origins 2017 conference (Early Earth and ExoEarths: origin and evolution of life), http://lifeorigins2017.ing.pan.pl/files/earlyearth2017/downloads/LifeOrigins2017_BOOK_OF_ABSTRACTS.pdf: 51–52.

Kruszewski, Ł., Fabiańska, M.J., Ciesielczuk, J., Segit, T., Orłowski, R., Motyliński, R., Moszumańska, I., Kusy, D. 2018. First multi-tool exploration of a gas-condensate-pyrolysate system from the environment of burning coal mine heaps: an *in situ* FTIR and laboratory GC and PXRD study based on Upper Silesian materials. Science of The Total Environment, **640–641**: 1044–1071.

Kruszewski, Ł., Fabiańska, M.J., Segit, T., Kusy, D., Motyliński, R., Ciesielczuk, J., Deput, E., 2019. Carbon-nitrogen compounds, alcohols, mercaptans, monoterpenes, acetates, aldehydes, ketones, SF_6, PH_3, and other fire gases in coal-mining waste heaps of Upper Silesian Coal Basin (Poland) – a re-investigation by means of in-situ FTIR extrernal database approach. Science of The Total Environment, **698**, doi: 10.1016/j.scitotenv.2019.134274.

Kuna-Gwoździewicz, P., 2013. Emission of polycyclic aromatic hydrocarbons from the exhalation zones of thermally active mine waste dumps. Journal of Sustainable Mining, **12**: 7–12.

Kynčlová, P., Hron, K., Filzmoser, P., 2017. Correlation between compositional parts based on symmetrical balances. Mathematical Geosciences, **49**: 777–796.

Lehmann, E.L., 1975. Nonparametrics: Statistical Methods Based on Ranks. Holden-Day, San Francisco.

Lewińska-Preis, L., Fabiańska, M.J., Parzentny, H., Kita, A., 2008. Geochemical characteristics of the macromolecular part of crude and biodesulphurised coal density fractions. Geochemistry, **68**: 279–293.

Li, C., Liang, H., Liang, M., Chen, Y., Zhou, Y., 2018. Soil surface Hg emission flux in coalfield in Wuda, Inner Mongolia, China. Environmental Science and Pollution Research, **25**: 16652–16663.

Lityński, T., 1971. Żyzność gleby i nawożenie (in Polish). PWN, Warszawa.

Mamindy-Pajany, Y., Hurel, Ch., Marmier, N., Roméo, M., 2009. Arsenic adsorption onto hematite and goethite. Comptes Rendus Chimie, **12**: 876–881.

Martinez, A.C., Ressler, D.E., 2001. Soil surface conditions of an active coal mine fire, Centralia PA. GSA Annual Meeting, November 5–8, 2001, Paper No. 98-0.

Meuser, H., 2013. Coal Mining Heaps (Sub-chapter 3.3.2). Mining Heaps (Chapter 3.2). In: Soil Remediation and Rehabilitation (eds. B.J. Alloway, J.T. Trevors, I. Colbeck, R.L. Crawford, W. Salomons): 59–69. Treatment of Contaminated and Disturbed Land. Springer Science+Business Media, Dordrecht, Germany.

Misz-Kennan, M., Fabiańska, M., 2010. Thermal transformation of organic matter in coal waste from Rymer Cones (Upper Silesian Coal Basin, Poland). International Journal of Coal Geology, **81**: 343–358.

Mocek, A. (ed.), 2015. Gleboznawstwo (in Polish). PWN, Warszawa.

Murray, J., Kirwan, L., Loan, M., Hodnett, B.K., 2009. In-situ synchrotron diffraction study of the hydrothermal transformation of goethite to hematite in sodium aluminate solutions. Hydrometallurgy, **95**: 239–246.

Nádudvari, Á., Fabiańska, M.J., Marynowski, L., Kozielska, B., Konieczyński, J., Smołka-Danielowska, D., Ćmiel, S., 2018. Distribution of coal and coal combustion related organic pollutants in the environment of the Upper Silesian Industrial Region. STOTEN, **628–629**: 1462–1488.

Nasdala, L., Pekov, I.V., 1993. Ravatite, $C_{14}H_{10}$, a new organic mineral species from Ravat, Tajikistan. European Journal of Mineralogy, **5**: 699–705.

Nelson, M., Chen, X.D., 2007. Survey of experimental work on the self-heating and spontaneous combustion of coal. GSA Reviews in Engineering Geology, **18**: 31–83.

Norton, J., Ouyang, Y., 2019. Controls and adaptive management of nitrification in agricultural soils. Frontiers in microbiology, **10**: 1931.

Novikova, S.A., Sokol, E.V., Novikov, I.S., Travin, A.V., 2015. Coal fires in the Kuznetsk Basin, Russia, chapter 19. In: Coal and Peat Fires: a Global Perspective (eds. G.B. Stracher, A. Prakash, E.V. Sokol): 510–541. Elsevier B.V.

Nowak, J., 2011. Wpływ stopnia przeobrażeń termicznych odpadów powęglowych na ługowanie substancji do środowiska (in Polish). Górnictwo i Geologia, **6**: 59–70.

Ou, J., Li, H., Yan, Z., Zhou, Y., Bai, L., Zhang, Ch., Wang, X., Chen, G., 2018. *In situ* immobilisation of toxic metals in soil using Maifan stone and illite/smectite clay. Scientific Reports, **8**: 4618.

Pałys, J., 1966. On genesis of brines in Upper Carboniferous in Upper Silesia (in Polish with English summary). Annales Societatis Geologorum Poloniae, **36**: 121–154.

Parfitt, R.L., Atkinson, R.J., 1976. Phosphate adsorption on goethite (-FeOOH). Nature, **264**: 740–742.

Parker, R.L., 1967. Data of Geochemistry, 6th ed. Chapter D. Composition of the Earth's Crust. U.S. Geological Survey Professional Paper, **440-D**.

Parzentny, H., 1994. Lead distribution in coal and coaly shales in the Upper Silesian Coal Basin. Geological Quarterly, **38** (1): 43–58.

Parzentny, H., Różkowska, A., Róg, L., 1999. Relationship between bed thickness, average ash content, and Zn and Pb content in coal in the Upper Silesian Coal Basin. Geological Quarterly, **43** (3): 365–374.

Parzentny, H.R., Lewińska-Preis, L., 2006. The role of sulphide and carbonate minerals in the concentration of chalcophile elements in the bituminous coal seams of a paralic series (Upper Carboniferous) in the Upper Silesian Coal Basin (USCB), Poland. Chemie der Erde, **66**: 227–247.

Pluta, I., Pindel, T., Janeczek, J., 2012. Aktywność izotopów radu w wodach kopalń Górnośląskiego Zagłębia Węglowe (in Polish). Wiadomości Górnicze, **63**: 351–357.

Querol, X., Zhuang, X., Font, O., Izquierdo, M., Alastuey, A., Castro, I., van Drooge, B.L., Moreno, T., Grimalt, J.O., Elvira, J., Cabañas, M., Bartroli, R., Hower, J.C., Ayora, C., Plana, F., López-Soler, A., 2011. Influence of soil cover on reducing the environmental impact of spontaneous combustion in coal waste gobs: a review and new experimental data. International Journal of Coal Geology, **85**: 2–22.

Raghad, M., Ameera, A., Munawar, I., 2016. Behavior of potassium in soil: a mini review. Chemistry International, **2**: 58–69.

Rietveld, H.M., 1967. Line profiles of neutron powder-diffraction peaks for structure refinement. Acta Crystallographica, **22**: 151–152.

Różański, Z., 2018. Fire hazards in coal waste dumps – selected aspects of the environmental impact. 2018 IOP Conference Series Earth and Environmental Science, **174**: 012013.

Ruefer, A.C., Johnson, E.A., McTaggart, E., Myers, E., Wilson, C.J.N., Wallace, P.J., 2018. Determining a Partition Coefficient for Water in Plagioclase for Rhyolitic Eruptions. AGU Fall Meeting 2018, abstract #V33D-0276.

Sánchez España, J., López Pamo, E., Santofimia, E., Aduvire, O., Reyes, J., Barettino, D., 2005. Acid mine drainage in the Iberian Pyrite Belt (Odiel watershed, Huelva, SW Spain): geochemistry, mineralogy and environmental implications. Applied Geochemistry, **20**: 1320–1356.

Schulthess, C.P., Ndu, U., 2017. Modeling the adsorption of hydrogen, sodium, chloride and phthalate on goethite using a strict charge-neutral ion-exchange theory. PLOS One, **12** (5), e0176743.

Schwertmann U., 1971. Transformation of hematite to goethite in soils. Nature, **232**: 624–625.

Seredin, V.V., Finkelman, R.B., 2008. Metalliferous coals: a review of the main genetic and geochemical types. International Journal of Coal Geology, **76**: 253–289.

Smoliński, A., Rompalski, P., Cybulski, K., Chećko, J., Howaniec, N., 2014. Chemometric Study of Trace Elements in Hard Coals of the Upper Silesian Coal Basin, Poland. The Scientific World Journal (Hindawi Publishing Corporation), article ID 234204, doi 10.1155/2014/234204

Sokol, E.V., Maksimova, N.V., Nigmatulina, E.N., Sharygin, V.V., Kalugin, V.M., 2005. Combustion metamorphism (in Russian). Publishing House of the SB RAS, Novosibirsk.

Sokol, E.V., Volkova, N.I., 2007. Combustion metamorphic events resulting from natural coal fires. GSA Reviews in Engineering Geology, **18**: 97–115.

Srebrodolskiy, B.I., 1989. Tainy Sezonnykh Mineralov (in Russian). Nauka, Moscow.

Stracher, G.B., 2007. The origin of gas-vent minerals: isochemical and mass-transfer processes. GSA Reviews in Engineering Geology, **18**: 91–96.

Szabó, D., Lovász, A., Weiszburg, T., Szakáll, S., Kristály, F., 2015. Ammonioalunite and adranosite-Al. New mineral species from the burning coal dumps of Pécs-Vasas, Hungary. Poster session presented at: 6th Mineral Sciences in the Carpathians Conference; 2015 May 16–19, Veszprém, Hungary.

Tobin-Janzen, T., Shade, A., Marshall, L., Torres, K., Beblo, C., Janzen, C., Lenig, J., Martinez, A., Ressler, D., 2005. Nitrogen changes and domain bacteria ribotype diversity in soils overlying the Centralia, Pennsylvania underground coal mine fire. Soil Science, **170**: 191–201.

Tripathi, N., Singh, R.S., Chaulya, S.K., 2012. Dump Stability and soil fertility of a coal mine spoil in indian dry tropical environment: a long-term study. Environmental Management, **50**: 695–706.

Tripathi, N., Singh, R.S., Nathanail, C.P., 2014. Mine spoil acts as sink of carbon dioxide in Indian dry tropical environment. Science of The Total Environment, **468–469**: 1162–1171.

Uddin, M.K., 2017. A review on the adsorption of heavy metals by clay minerals, with special focus on the past decade. Chemical Engineering Journal, **308**: 438–462.

Ugwu, I.M., Sherman, D.M., 2017. Irreversibility of sorption of cobalt to goethite (-FeOOH) and dispartities in dissolution of aged synthetic Co-goethite. Chemical Geology, **467**: 168–176.

Upadhyay, N., Verma, S., Singh, A.P., Devi, S., Vishwakarma, K., Kumar, N., Pandey, A., Dubey, K., Mishra, R., Tripathi, D.K., Rani, R., Sharma, S., 2016. Soil ecophysiological and microbiological indices of soil health: a study of coal mining site in Sonbhadra, Uttar Pradesh. Journal of Soil Science and Plant Nutrition, **16**: 778–800.

Wagner, M., 1980. Przemiany termiczne węgla kamiennego w strefach pożarów hałd kopalnianych (in Polish). Zeszyty Naukowe Akademii Górniczo-Hutniczej – Geologia **6**: 5–14.

Witzke, T., 1996. Die Minerale der brennenden Halde der Steinkohlengrube "Deutschland-schacht" in Oelsnitz bei Zwickau. Aufschluss, **47**: 41–48.

Žáček, V., Opluštil, S., Máyová, A., Meyer, F.R., 1995. Die Mineralien von Kladno in Mittelböhmen, Tschechische Republik. Mineralien-Welt, **6**: 13–30.

Zając, E., Zarzycki, J., 2013. Wpływ aktywności termicznej zwałowiska odpadów węgla kamiennego na rozwój roślinności (in Polish). Rocznik Ochrona Środowiska, **15**: 1862–1880.

Zawadzki, S., (ed.), 1999. Gleboznawstwo (in Polish). PWRiL, Warszawa.